# Observational evidence of Alfvén wings at the Earth

E. Chané,[1] J. Saur,[1] F. M. Neubauer,[1] J. Raeder,[2] and S. Poedts[3]

Received 16 February 2012; revised 3 August 2012; accepted 3 August 2012; published 15 September 2012.

[1] The solar wind at the orbit of the Earth is usually strongly super-Alfvénic and super-fast, causing a bow-shock to be formed upstream of the Earth's magnetosphere. We here present observational evidence that during 24 and 25 May 2002, the solar wind at the Earth was sub-Alfvénic (with an Alfvén Mach number as low as 0.4 in the rest frame of the Earth) and was therefore sub-fast for time periods of up to four hours. The low Alfvén Mach number implies that the Earth's bow-shock disappeared and two Alfvén wings formed. These Alfvén wings are two structures on both the East and West side of the Earth's magnetosphere, where the solar wind plasma is decelerated and the magnetic field direction changes. We present observations of the Geotail spacecraft, which are consistent with Geotail entering the foot of one of these Alfvén wings. We estimate that these wings reached an extension of 600 $R_E$. Even though Alfvén wings are present at several moons in the solar system (e.g., Io, Europa, Enceladus) and are likely to occur at some extrasolar planets, this is the first time that they are observed at the Earth. We also study how the Earth is affected by this transition from a super-fast to a sub-Alfvénic environment and how the Alfvén wings are affected by the constantly varying solar wind. The sub-Alfvénic solar wind is due to very low density in the solar wind. While the solar wind Alfvén Mach number was very low, the magnetosphere was geomagnetically extremely quiet. Whereas the SYM-H index indicates a recovery phase from a small to moderate magnetic storm; the AL and AU indices show no substorm activity. In addition, there was almost no auroral activity.

**Citation:** Chané, E., J. Saur, F. M. Neubauer, J. Raeder, and S. Poedts (2012), Observational evidence of Alfvén wings at the Earth, *J. Geophys. Res.*, *117*, A09217, doi:10.1029/2012JA017628.

## 1. Introduction

[2] The interaction between the solar wind and the Earth's magnetosphere is usually such that the super-Alfvénic solar wind plasma (with an Alfvén Mach number, $M_A$, of approximately 11 [see *Schunk and Nagy*, 2000]) is suddenly decelerated at the bow-shock (typically located at 15 $R_E$ [see *Fairfield*, 1971]) where the magnetic field strength and orientation also experience a sudden change. In the magnetosheath, the slower plasma is then deviated around the Earth's magnetopause (typically located at 11 $R_E$ [see *Fairfield*, 1971]). Inside the magnetopause, the magnetic field of the Earth is deformed by the interaction with the solar wind, causing compressed field lines on the day side and elongated field lines on the night side forming the magnetotail. The Earth's magnetosphere nearly always displays such a configuration since the solar wind Alfvén Mach number ($M_A$) and fast magnetosonic Mach number ($M_f$) are almost always larger than one.

[3] Plasma environments with $M_A < 1$ and $M_f < 1$ are not known for planets in our solar system, but are expected to occur at extrasolar planets [see, e.g., *Shkolnik et al.*, 2003; J. Saur et al., submitted manuscript, 2012] and observed at planetary satellites embedded in the plasma of their parent planet's magnetosphere [see, e.g., *Neubauer*, 1998; *Kivelson et al.*, 2004, and references therein]. In this case neither a bow-shock nor a magnetosheath is present, but instead two Alfvén wings are generated (see Figure 1, top). As was first shown by *Drell et al.* [1965] for the weak interaction case, Alfvén waves generated by a plasma flow encountering a conducting obstacle propagate along the magnetic field lines in the rest frame of the plasma (in both directions); They are simultaneously convected by the plasma flow, and, as a result, an Alfvén wing forms on both sides of the obstacle. The velocity and the magnetic field of the plasma flow can be strongly altered by the Alfvén wings. An extension for full nonlinear amplitudes has been given by *Neubauer* [1980].

[4] In this article, we present observational evidence that the Earth's near space environment was exposed to sub-Alfvénic and sub-fast solar wind conditions ($M_A < 1$ and

[1]Institut für Geophysik und Meteorologie, Universität zu Köln, Cologne, Germany.
[2]Space Science Center, University of New Hampshire, Durham, New Hampshire, USA.
[3]Centrum voor Plasma-Astrofysica, Katholieke Universiteit Leuven, Leuven, Belgium.

Corresponding author: E. Chané, Institut für Geophysik und Meteorologie, Universität zu Köln, Albertus-Magnus-Platz, DE-50923 Cologne, Germany. (chane@geo.uni-koeln.de)


0148-0227/12/2012JA017628

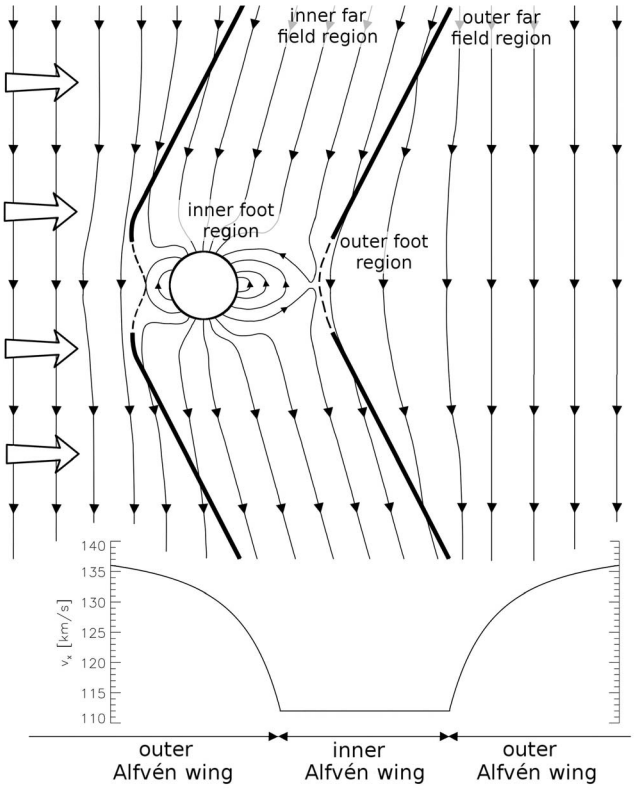


**Figure 1.** (top) Sketch of Ganymede and its magnetic field lines (thin lines), where the external magnetic field and the dipole moment are parallel to each other. The boundary between the inner part of the Alfvén wings and the outer part is represented by bold lines. Ganymede, located in the magnetosphere of Jupiter, is embedded in a sub-Alfvénic plasma flow (coming from the left on the sketch), but also subsonic in contrast to the situation at Earth discussed in this paper, and possesses an internal dipole field. (bottom) Plasma velocity profile across the Alfvén wing.

$M_f < 1$) on 24 and 25 May 2002. It is thus expected to undergo a complete transition, to lose its bow-shock and magnetosheath, and to develop Alfvén wings. We also present in detail the expected geometry of the magnetosphere during this period and study how the Alfvén wings alter the incoming plasma flow and the magnetic field. In addition, we show evidence of Alfvén wing crossings by the spacecraft Geotail.

[5] A study of the Earth's magnetosphere embedded in a sub-Alfvénic solar wind was already conducted by *Ridley* [2007], who performed numerical experiments with a very strong solar wind magnetic field pointing exactly southward ($B_z = -45$ nT and $-60$ nT to obtain $M_A = 0.9$ and 0.7, respectively). The solar wind conditions on 24 and 25 May 2002 were very different, with a more usual solar wind magnetic field strength of 9.8 nT on average, mostly confined to the equatorial plane, but with a very low density.

[6] Before we present data of the Earth's plasma and magnetic field environment for $M_A < 1$, we discuss some basic physics of the Alfvén wings in the next section, using Jupiter's moon Ganymede as a prime example. In section 3, we discuss the relevant characteristics of the magnetospheric configuration on 24 and 25 May 2002: upstream conditions, positions of the magnetopause and bow-shock, the influence of the Alfvén wings on the plasma, and the temporal variation of the Alfvén wings. In section 4, we identify in which region of the magnetosphere Geotail was located during this period and provide evidence that it crossed one of the Alfvén wings. In section 5, we study the effect of the transition to a sub-Alfvénic configuration of the magnetosphere on the aurorae and geomagnetic indices. Finally, our conclusions are presented in section 6.

## 2. Physics of Alfvén Wings

[7] The Alfvén wings of the Jovian moon Ganymede are directly relevant for this study because they are well known, fairly well understood, and have been studied multiple times with in situ measurements and plasma simulations [e.g., *Kivelson et al.*, 1996; *Jia et al.*, 2008]. Like the Earth, but unlike the other moons of the solar system, Ganymede displays an intrinsic magnetic field. It is constantly exposed to a sub-Alfvénic plasma, which makes it so interesting for our study. However, Ganymede's environment differs from the Earth's environment. The magnetic field of the incoming plasma, for instance, points approximately southward for Ganymede, which is not the case upstream of the Earth for the present study. In addition, while the incident plasma at Ganymede is subsonic, it is strongly supersonic in our case at the Earth.

[8] Figure 1 shows an idealized sketch of the Alfvén wings at Ganymede. Figure 1 (top) shows how the magnetic field is affected by Ganymede, and Figure 1 (bottom) shows how the plasma speed changes. One can see that not only Ganymede and Ganymede's closed field lines region constitute an obstacle to the flow, but that the plasma is also decelerated in the two long structures located north and south of the moon: these are the Alfvén wings of Ganymede. The wings are caused by Alfvén waves generated by the obstacle and form a stationary wavefield in the rest frame of Ganymede. At some distance from Ganymede the amplitudes of slow and fast modes, which are also generated by the interaction, have significantly decreased and thus the Alfvén wave amplitude becomes constant. Therefore Alfvén wings are translation-invariant and can be very long structures.

[9] In Figure 1 we also define the different regions of the Alfvén wings. The inner part of the Alfvén wing is the region where the Alfvén waves generated by the obstacle (in the area of the ionosphere with open field lines) propagate. These waves travel along the field lines with a velocity $\pm\mathbf{v_A} = \pm\mathbf{B}/(\mu_0\rho)^{\frac{1}{2}}$ in the rest frame of the unperturbed plasma (where $\mathbf{B}$ is the magnetic field, $\rho$ the mass density and $\mu_0$ the vacuum permeability) and are also advected by the plasma flow (velocity $\mathbf{v}$). As a result, in the frame of the obstacle, the Alfvén wings point in the direction of the Alfvén characteristics $\mathbf{C_A^+}$ and $\mathbf{C_A^-}$ (where $\mathbf{C_A^\pm} = \mathbf{v} \pm \mathbf{v_A}$). This has been verified for different moons by numerous observations [see, e.g., *Kivelson et al.*, 1996; *Khurana et al.*, 1998, 2007] and simulations [e.g., *Linker et al.*, 1991; *Schilling et al.*, 2007; *Jacobsen et al.*, 2007; *Jia et al.*, 2008]. In Figure 1 the Alfvén wings point approximately north and south and are symmetric with respect to the equatorial plane. This does not have to be the case at the Earth, where,


**Figure 2.** (top) Solar wind density measured by SOHO (black), ACE (red), WIND (green) and Genesis (blue). (middle) Solar wind Alfvén Mach number calculated from ACE (red) and WIND (green) measurements. (bottom) Solar wind plasma $\beta$ calculated from ACE (red) and WIND (green) measurements. The time interval with a very low density and a very low Alfvén Mach number (mainly less than one) is highlighted with the blue background color.

depending on **v** and $\mathbf{v_A}$ in the solar wind, the wings could be very asymmetric and point, e.g., to the flanks of the planet.

[10] As can be seen in Figure 1 (bottom), in the inner part of an Alfvén wing, the velocity displays a low value, which is a constant on the sketch because constant effective ionospheric conductances were assumed.

[11] The outer part of the wing is the region located around the inner part. In this region the incoming plasma is affected by the presence of the inner wing, which acts as an obstacle to the plasma. The plasma is decelerated upstream of the inner Alfvén wings and re-accelerated downstream to the background value (see Figure 1, bottom). Furthermore, the plasma is accelerated on the flanks of the Alfvén wings (away from the plane of the drawing, not shown on the sketch) and, in extreme cases, reaches speeds up to twice the incident flow speed, just outside of the inner wing.

[12] The magnetic field in the Alfvén wings is also affected in a similar way: it displays a constant value in the inner part of the wings (at least in the far field region) but is also affected in the outer part. The higher the ionospheric conductance, the stronger **B** and **v** are affected by the wings. In case of an infinite Pedersen conductance, **B** and **v** are perfectly aligned with the wings axis $\mathbf{C_A^+}$ and $\mathbf{C_A^-}$. Outside the inner wing the magnetic field components perpendicular to the wing axis vary according to a two-dimensional dipole, i.e. proportional to the inverse square of the distance from the wing axis. The component parallel to the wing axis enforces the constancy of the magnetic field magnitude.

[13] Far from the ionosphere, in the Alfvén wing, is a region where the interactions are purely Alfvénic because: 1) the slow mode waves generated by the obstacle are not present since they do not propagate in the direction of the Alfvén wing and 2) the amplitudes of the fast mode waves, which propagate in every direction, become much lower than the ones of the Alfvén waves far from the obstacle because of the spatial decay with distance from the Earth. This part of the Alfvén wing is called the far field region. On the contrary, close to the obstacle, but still outside the closed field line magnetospheric region, is a region where the slow mode waves and fast mode waves play an important role and tend to perturb the Alfvén wing: we call it the "foot region" of the Alfvén wing.

## 3. The Earth's Magnetosphere on 24 and 25 May 2002

[14] In the present section, we show that the solar wind upstream of the Earth on 24 and 25 May 2002 was sub-Alfvénic for long periods of time (up to four hours) due to an unusually low plasma density. We therefore expect the Earth to develop Alfvén wings similar to the ones of Ganymede. We study their expected geometry, extension and time variability.

### 3.1. Solar Wind Density and Alfvén Mach Number

[15] For Alfvén wings to be generated, the incoming plasma must have a low Alfvén Mach number and a low fast magnetosonic Mach number (ideally below one). In the present study, these two Mach numbers are almost equal. This is the case, as we show in the Appendix, because the plasma $\beta$ in the solar wind (see Figure 2, bottom) is very low for the period of interest. When the fast magnetosonic Mach number is clearly above one, due to the presence of the bow-shock, the shocked solar wind will preclude the formation of clearly defined Alfvén wings, whereas an admixture of Alfvén waves is still expected.

[16] As can be seen in Figure 2 (middle), during 24 and 25 May 2002, the solar wind Alfvén Mach number was very low, namely less than two for a period of about 42 hours and less than one for several periods lasting up to four hours. The Alfvén Mach number was calculated for two spacecraft located in the solar wind: ACE and WIND. More

specifically, the plasma instrument SWEPAM [*McComas et al.*, 1998] was used to obtain the density and the velocity at ACE while the magnetometer MAG [*Smith et al.*, 1998] provided the magnetic field. For the WIND spacecraft, the density and velocity were measured by the 3DP instrument [*Lin et al.*, 1995] and the magnetic field by the magnetometer MFI [*Lepping et al.*, 1995]. It can be seen in the figure that the values obtained by the two spacecraft are in good agreement, and that both spacecraft measured long time intervals of sub-Alfvénic flow during 24 and 25 May 2002.

[17] The low Alfvén Mach number was not due to an abnormally low plasma velocity, but due to an unexpectedly high Alfvén velocity. The Alfvén velocity was high because the solar wind density was very low. As one can see in Figure 2 (top) (where the period of very low density is highlighted in blue), the solar wind density was below 0.5 $cm^{-3}$ for at least 40 hours and below 0.1 $cm^{-3}$ for several hours. Four spacecraft provided independent and consistent measurements of the solar wind density in the near Earth orbit: SOHO, ACE, WIND and Genesis, of which the instruments CELIAS [*Hovestadt et al.*, 1995], SWEPAM [*McComas et al.*, 1998], 3DP [*Lin et al.*, 1995] and GIM [*Barraclough et al.*, 2003] were used, respectively. All spacecraft measured density values below 0.1 $cm^{-3}$.

[18] The Alfvén Mach number and plasma $\beta$ could only be determined from ACE's and WIND's measurements, since SOHO and Genesis were not equipped with a magnetometer.

[19] Very low density conditions in the solar wind are rare, but not unheard of. The most famous low density event is probably "the day the solar wind almost disappeared", which occurred on 11 May 1999. During this event, the solar wind density dropped below 1 $cm^{-3}$ for more than one day [*Le et al.*, 2000] and reached values as low as $\sim$0.2 $cm^{-3}$ [*Farrugia et al.*, 2000]. Due to the low ram pressure, the magnetopause and bow-shock expanded and were observed by Geotail 8 $R_E$ further out than usual positions [*Terasawa et al.*, 2000]. The bow-shock was even crossed by Lunar Prospector at 58 $R_E$ [*Fairfield et al.*, 2001] and by the WIND spacecraft at 53 $R_E$. The subsolar bow-shock position was estimated to be at 58 $R_E$ [*Le et al.*, 2000].

### 3.2. Position of the Magnetopause and of the Bow-Shock

[20] The position of the bow-shock and of the magnetopause are tightly linked to the ram pressure of the solar wind. For periods of high solar wind ram pressure, the magnetosphere is compressed and the bow-shock as well as the magnetopause are located closer to the Earth (as close as 6.8 $R_E$ and 5 $R_E$, respectively [see *Russell et al.*, 2000]), whereas for periods of low solar wind ram pressure, the bow-shock and magnetopause are far from the Earth (for "the day the solar wind almost disappeared" more than 58 $R_E$ and 19 $R_E$, respectively [see *Le et al.*, 2000; *Terasawa et al.*, 2000]). During 24 and 25 May 2002, the solar wind ram pressure was very low due to the unusually low density. Using the empirical model of *Shue et al.* [1998] to estimate the position of the magnetopause during this period, one finds magnetopause standoff distances as high as 22 $R_E$ (for example at 10:04UTC on 25 May 2002 when the density was as low as 0.05 $cm^{-3}$ and the velocity as high as 380 km/s). However, it should be mentioned that this empirical model was not developed for such extremely low solar wind density values and may not be directly applicable to this event.

[21] During the time periods of very low density, the magnetic pressure in the solar wind is larger than the ram pressure (low $M_A$; see Figure 2, middle). In this case, the size of the magnetosphere is determined not only by the ram pressure but mostly by the magnetic pressure of the solar wind. The magnetopause standoff distance can then be very roughly estimated by $\left(\frac{2B_0^2}{\mu_0} / \left(\rho_{sw} v_{sw}^2 + \frac{B_{sw}^2}{2\mu_0}\right)\right)^{1/6}$, where $B_0$ is the equatorial surface magnetic field of the Earth; $\rho_{sw}$, $v_{sw}$ and $B_{sw}$ the mass density, plasma speed and magnetic field in the solar wind, respectively. Values as high as 18 $R_E$ are found for this time interval.

[22] Due to the low ram pressure, the bow-shock also moves away from the Earth. Actually, since the Alfvén Mach number and the fast magnetosonic Mach number are even below one for some time periods, the bow-shock formally moves away to infinity. Consequently, during these periods, the Earth has neither a bow-shock, nor a magnetosheath with shocked solar wind.

### 3.3. Characteristics of the Alfvén Wings

[23] We have shown that for 24 and 25 May 2002 solar wind measurements are consistent with the formation of Alfvén wings at the Earth for several long time periods. We here discuss in detail the theoretical expectations for the geometry, the extent and time variability of these Alfvén wings. Idealized sketches of the typical Alfvén wings during these periods, showing the anticipated general geometry, are given in Figure 3 and in Figure 4 (right). These sketches depict that, in the absence of a bow-shock, the solar wind plasma should reach the magnetopause and that two Alfvén wings should form. While in Figure 3 a very simplified three-dimensional sketch of the Alfvén wings and of the magnetic field lines is provided, a two-dimensional drawing with magnetic field lines and velocity streamlines is presented in Figure 4. The orientation of the wings can be calculated from the solar wind measurements and is given by $\mathbf{C_A^{\pm}} = \mathbf{v} \pm \mathbf{v_A}$. For instance on 24 May 2002 at 23:30 UTC, the directions of the Alfvén wings were: (−0.82, 0.57, 0.03) and (0.13, −0.94, 0.32) in GSE coordinates. In this system, the X-axis points to the Sun, the Z-axis to the ecliptic north pole, and the Y-axis completes the right-handed coordinate system. Eleven hours later, on 25 May 2002 at 10:30 UTC their directions were: (−0.93, 0.3, 0.21) and (−0.15, −0.78, −0.61). In addition, the analytical model of *Neubauer* [1980] can be used to derive the magnetic field and the plasma velocity in the Alfvén wings from the upstream condition, knowing the conductance of the ionosphere; using for instance equations (14), (15) and (26) from *Neubauer* [1980] and equation (A10) from *Saur et al.* [1999].

[24] The topology of the Earth's magnetosphere in this study is very different from the usual configuration (see Figure 4, left) and also displays some differences compared to Ganymede (see Figure 1, top). On the sketches one can see that: 1) the wings point to the side of the Earth's magnetosphere (there is a dawn wing and a dusk wing); 2) the two wings are not symmetric: while the dawn wing points to the side, in a direction almost perpendicular to the solar wind velocity, the dusk wing points more tailward. This is somewhat different from what is observed at Ganymede, where

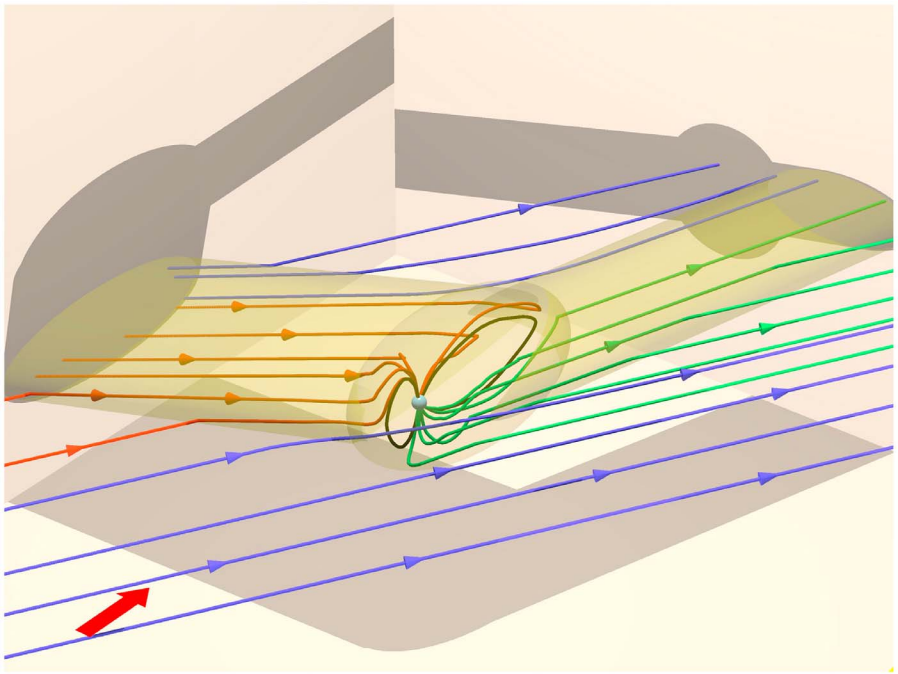

**Figure 3.** Three dimensional sketch of the Alfvén wings on 24 and 25 May 2002. The magnetic field lines are shown in red when connected to the northern ionosphere, in green when connected to the southern ionosphere, in black for the closed field lines and in blue when not connected to the Earth's ionosphere. The two Alfvén wings and the closed field line region are represented by the yellow semitransparent areas. These regions are projected (in dark gray) on three planes (X = −210, Y = −180 and Z = −95 in GSE) to show the geometry of the wings. The light blue sphere in the middle symbolizes the Earth (not to scale: R = 3 $R_E$). The direction of the incoming solar wind is shown by the flat red arrow.

the wings are almost symmetric. This is because the background magnetic field and velocity are approximately perpendicular at Ganymede (exactly perpendicular in Figure 1), while they are not perpendicular at the Earth during the period of interest.

[25] During 24 and 25 May 2002, the ionospheric Pedersen conductance was higher (International Reference Ionosphere model [*Bilitza*, 2001; *Bilitza and Reinisch*, 2008]) than the Alfvén conductance in the solar wind (which was unusually low due to the unusually high Alfvén speed). Therefore the magnetic field lines in the wings are expected to be almost aligned with the axis of the wings (strong interaction). Some of the magnetic field lines are connected to the Earth ionosphere on one side and to the solar wind on the other side: the field lines of the dawn Alfvén wing connect to the northern hemisphere, while the field lines of the dusk wing are linked to the southern hemisphere (illustrated in Figure 3). This means that the usual north and south lobe of the magnetotail are not present and were progressively replaced by the dawn and the dusk Alfvén wings, respectively. The progressive transformation of the lobes in Alfvén wings can clearly be seen in the numerical study of *Ridley* [2007]; see his Figure 7.

[26] In the inner part of the wings, the plasma is decelerated. The higher the conductance in the terrestrial polar ionosphere, the lower the plasma speed in the wing. Moreover, according to theory, the plasma speed is lower in the dawn wing (due to its orientation) than in the dusk wind. In Figure 4, using the *Neubauer* [1980] model and assuming a constant effective Pedersen conductance of 10 S, we have calculated that the plasma speeds were 43% and 70% of the solar wind speed in the dawn and dusk wing, respectively. The effective conductance used here is given by the real conductance weighted by some small geometric factor accounting for the field geometry, since the field is not homogeneous here, as it is in *Neubauer* [1980]. For more details, see *Wolf-Gladrow et al.* [1987] and *Neubauer* [1998].

[27] Since the solar wind Alfvén Mach number is less than one for time intervals up to four hours, Alfvén waves can be continuously generated throughout this time interval. Consequently, a long wing structure can be formed. Because it propagates with the Alfvén velocity, in four hours an Alfvén wing can travel more than 600 $R_E$.

[28] One of the Alfvén wings points in the direction $\mathbf{C_A^-} = \mathbf{v} - \mathbf{v_A}$, which is, for the period of interest (when $M_A < 1$), approximately in the dawn direction (depicted in Figure 3), even though this direction strongly varies with time because of the ever-changing upstream conditions. Due to the orientation of $\mathbf{v}$ and $\mathbf{v_A}$ in the solar wind during this period, the Y-component of $\mathbf{C_A^-}$ (GSE coordinate system) is strongly negative; while the Z-component negative, but not as strongly as the Y-component; and the X-component low (negative or positive). On average, $\mathbf{C_A^-}$ points toward 5:30 LT; but can point in directions as far as 3:30 LT and 7:40 LT. Due to the ever-changing direction of $\mathbf{C_A^-}$, the wing is not a straight line (see our expectations in Figure 4). The sketch illustrates how the wing changes its orientation at 10:45 UTC from pointing slightly upstream in the dawn direction to

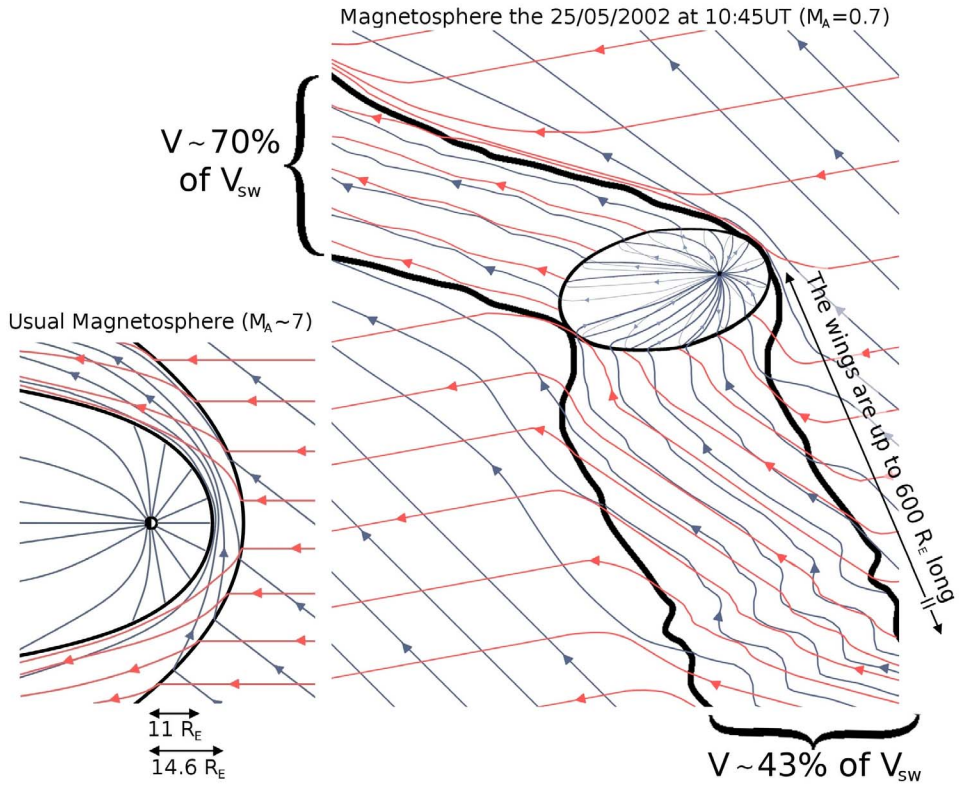


**Figure 4.** Sketch of the interaction between the solar wind and the Earth's magnetosphere seen from the north. The magnetic field is shown in blue, the velocity in red. (left) Nominal interaction; the bow-shock and the magnetopause are represented by bold black lines. (right) typical interaction during 24 and 25 May 2002 (the sketch was drawn for the data recorded by ACE at 10:45UTC 25 May 2002). There is no bow-shock, the magnetopause is located further from the Earth and two Alfvén wings are present (represented by the black bold straight lines). The magnetic field and velocity of the solar wind are strongly affected by the Alfvén wings (an effective ionospheric conductance of 10 S was assumed).

pointing slightly downstream. Therefore, the magnetic field and velocity streamlines in the inner region of the wing are no straight lines unlike, for example, in Figure 1).

[29] On the other side of the Earth, the other wing points in the direction $\mathbf{C}_\mathbf{A}^+ = \mathbf{v} + \mathbf{v}_\mathbf{A}$. The unit vector which describes the direction of this wing has a small positive Z-component. It displays a strong negative X-component and a small positive Y-component (see Figure 3). On average, this wing points toward 22:20 LT. For geometrical reasons ($\mathbf{v}$ and $\mathbf{v}_\mathbf{A}$ are approximately in the same direction) this wing does not vary with time as strongly as the other wing, in the direction ranging between 21:25 LT and 22:55 LT.

## 4. Alfvén Wing Crossings

[30] In the previous section, we used theoretical considerations and solar wind measurements to argue for the presence of Alfvén wings at the Earth on 24 and 25 May 2002. We now try to find direct evidence for the presence of these wings by studying Geotail's data. Figure 5 shows the orbit of Geotail and the positions of the magnetopause and bow-shock for three different solar wind conditions (nominal, low and high density). The empirical models of *Shue et al.* [1998] and *Chao et al.* [2002] were used to determine the positions of the magnetopause and of the bow-shock, respectively. This figure shows that Geotail was close to the Earth, probably in the closed magnetic field line region, until the evening of 22 May 2002. It then remained for several days at large radial distances, mostly on the afternoon side, in a region which lies in the magnetosheath for calm upstream conditions, and in the case of a compressed magnetosphere lies in the solar wind. We will see that, during that time, Geotail also penetrated the inner and outer foot region of an Alfvén wing (located on the dusk side of the Earth). During 25 May 2002, it moved back in the closed magnetic field line region, namely into the magnetotail.

[31] In this section, we use Geotail measurements to identify the theoretically expected regions (e.g., solar wind, magnetosheath, Alfvén wing). We start with 23 May 2002 when the solar wind Alfvén Mach number is high (approximately 10) and compare our results with empirical models for the position of the bow-shock [*Chao et al.*, 2002] and of the magnetopause [*Shue et al.*, 1998]. We then continue our analysis for 24 and 25 May 2002 where the Alfvén Mach number becomes very low. The empirical models available in the literature are less likely to give very accurate results for such unusual solar wind values. During this time period Geotail might have left the closed magnetic field line region

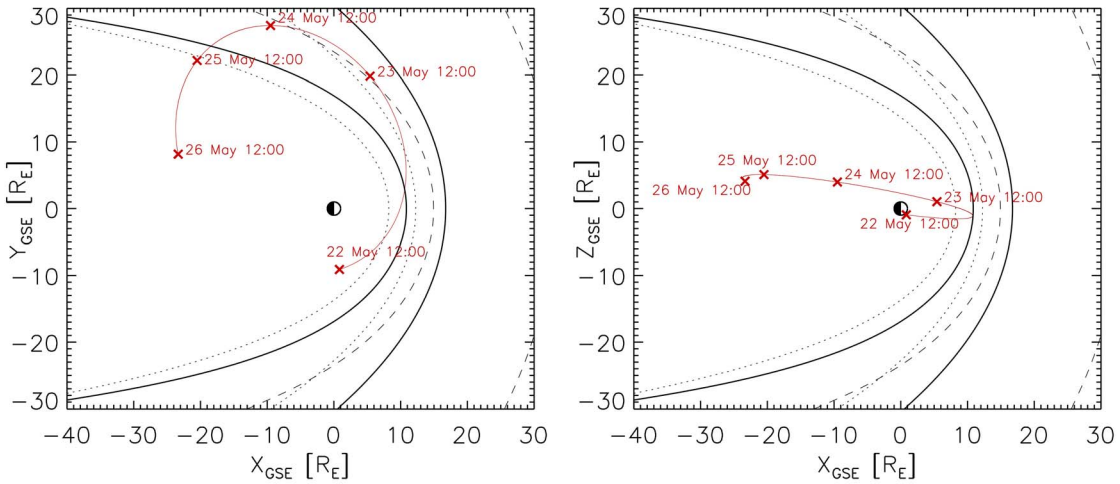


**Figure 5.** Position of Geotail. The locations of the magnetopause and bow-shock are shown by bold black lines for nominal solar wind conditions, by dashed black lines for a low density solar wind ($\rho$ = 0.6 cm$^{-3}$, $M_A$ = 2); and by dotted black lines for a high density solar wind ($\rho$ = 20 cm$^{-3}$, $M_A$ = 10). For the position of the magnetopause and bow-shock, the empirical models of *Shue et al.* [1998] and *Chao et al.* [2002] were used, respectively.

and entered the foot of the Alfvén wing located on the dusk side. At the end of 25 May 2002, when the solar wind Alfvén Mach number returns to higher values, our analysis is expected to be in good agreement with the empirical models again.

[32] Figure 6 shows the in situ data measured by ACE and Geotail. Geotail possesses two plasma monitors (CPI [see *Frank et al.*, 1994] and LEP [see *Mukai et al.*, 1994]). Since they both display slightly different data and do not have the same data gaps, we show data from these two plasma monitors in Figure 6 (see the fifth through seventh panels where the velocity is given). The magnetic field at Geotail (first through third panels) is measured by MGF [*Kokubun et al.*, 1994].

[33] When Geotail is in the solar wind, ACE and Geotail measurements should be very similar. These time periods are abbreviated SW in Figure 6. One can see that the magnetic field measurements are almost identical for the two spacecraft and that the plasma monitors give similar values. It means that, during these time periods, the Earth's magnetosphere was in a highly compressed configuration due to the high solar wind ram pressure (see Figure 5). This interpretation is in general agreement with the empirical models of *Shue et al.* [1998] and *Chao et al.* [2002], which predict that Geotail is either in the solar wind or in the magnetosheath (but close to the bow-shock) during these time periods. For example, during the second SW interval of Figure 6 (around 4:00 UTC on 23 May 2002), the empirical models predict that Geotail is 52% of the time in the solar wind and 48% in the magnetosheath. When the spacecraft is predicted to be in the magnetosheath, the distance to the bow-shock is on average 0.9 $R_E$ and never larger than 2.1 $R_E$. This comparison with the empirical models supports our interpretation of the data that Geotail was located in the solar wind for these time periods.

[34] When Geotail is located in the magnetosheath, the measured magnetic field should be stronger and the plasma speeds lower than at ACE (since a bow-shock is located between the two spacecraft). These periods are abbreviated MSH in Figure 6. As can be seen in Figure 5, Geotail is expected to be located in the magnetosheath (assuming nominal solar wind conditions) during these periods. Again, we can check whether the empirical models agree with our interpretation. For example, for the third MSH interval of Figure 6 (around 9:00UTC on 23 May 2002) these models are in complete agreement with our interpretation. During the fourth MSH interval (around 14:00UTC on 23 May 2002) Geotail is found to be located 88.5% of the time in the magnetosheath and 11.5% in the solar wind (but close to the bow-shock, never further than 4.2 $R_E$). This is in very good agreement with our interpretation of the data.

[35] At 5:00 UTC and 12:00 UTC on 23 May 2002, the variations at Geotail that we identify as a bow-shock crossing from the solar wind into the magnetosheath correspond to a sudden decrease of the density of the incoming solar wind measured by ACE. Due to this density decrease, the bow-shock moves away from the Earth, which explains the bow-shock crossing at Geotail. In contrast, the sharp transition around 16:00 UTC on 23 May 2002 that we identify as a bow-shock crossing from the magnetosheath into the solar wind happens when the solar wind density measured by ACE suddenly increases. This implies an inward moving bow-shock and agrees with our interpretation. The other bow-shock crossings by Geotail were not triggered by sharp density changes in the incoming solar wind.

[36] When Geotail is located on the closed magnetic field lines of the Earth, the measured plasma speed should be very low. In addition, the magnetic field can have a very different orientation depending on the exact location of Geotail in the magnetosphere and on how much the Earth's closed field lines are deformed by the solar wind. In Figure 6, these time periods are abbreviated MSP. The X-component of the magnetic field at Geotail is positive during these intervals (while negative at ACE). This is consistent with Geotail

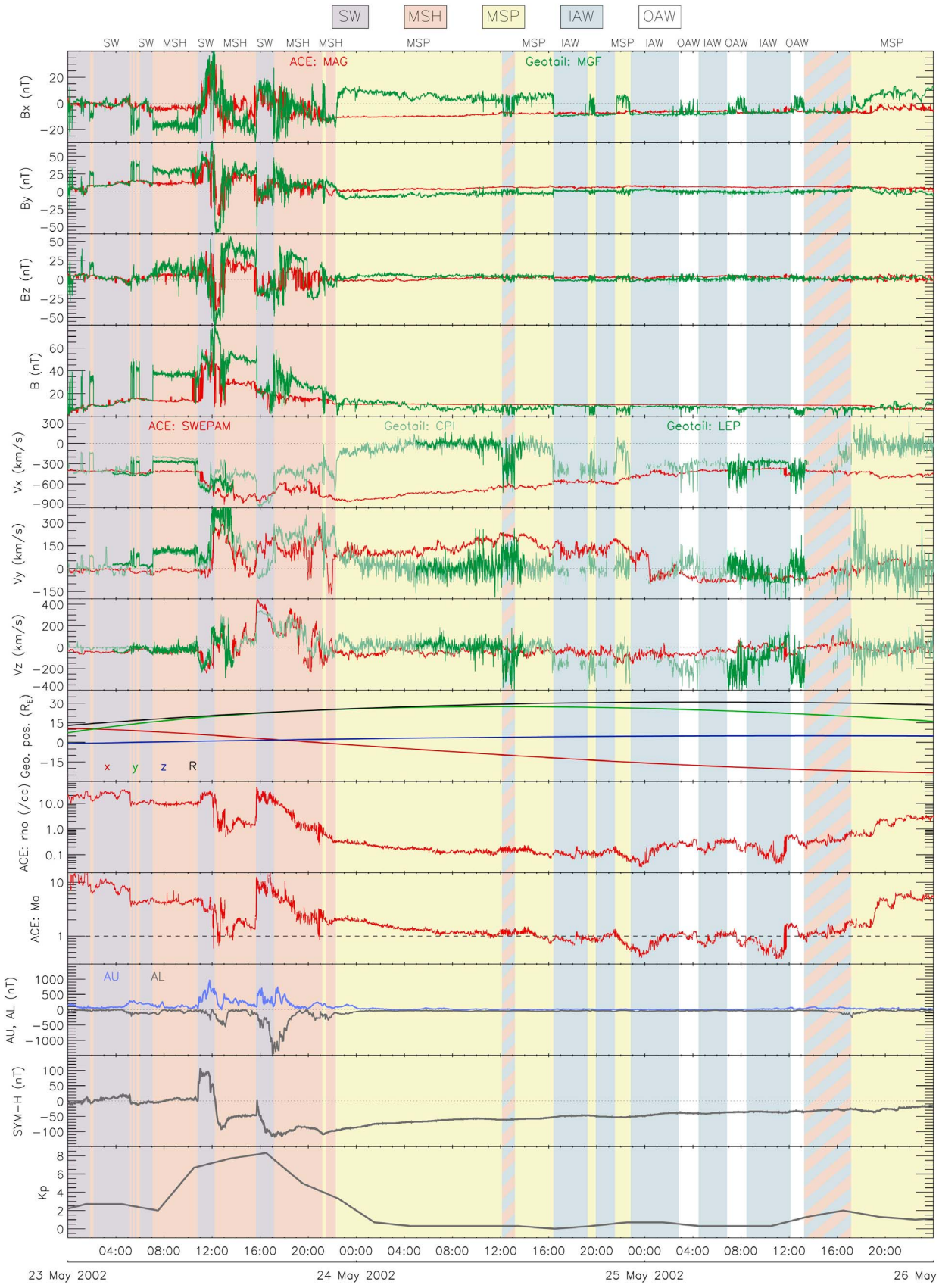
SW
MSH
MSP
IAW
OAW
ACE: MAG
Geotail: MGF
Bx (nT)
By (nT)
Bz (nT)
B (nT)
ACE: SWEPAM
Geotail: CPI
Geotail: LEP
Vx (km/s)
Vy (km/s)
Vz (km/s)
Geo. pos. (R_E)
x y z R
ACE: rho (/cc)
ACE: Ma
AU AL
AU, AL (nT)
SYM−H (nT)
Kp
04:00 08:00 12:00 16:00 20:00 00:00 04:00 08:00 12:00 16:00 20:00 00:00 04:00 08:00 12:00 16:00 20:00
23 May 2002
24 May 2002
25 May 2002
26 May

**Figure 6**

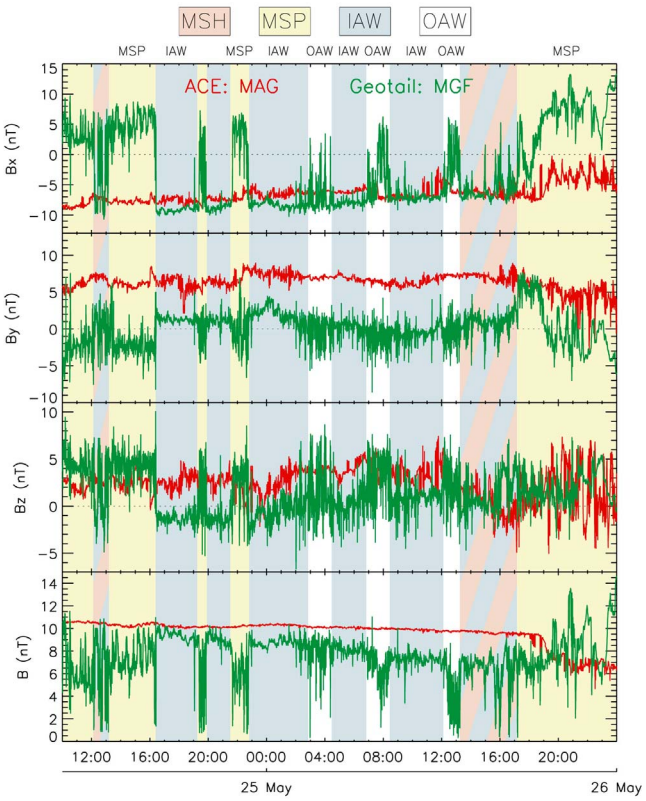


**Figure 7.** Same as the first through fourth panels from Figure 6, but zoomed in on the region of interest where Alfvén wings are present.

being on the far dusk side of the magnetosphere, on strongly bent magnetic field lines. We note that from 23 May 2002 at 22:15 UTC Geotail does not enter the magnetosheath (which is not expected to exist when $M_A < 1$) or the solar wind. This corresponds to a very extended magnetosphere (see Figure 5) caused by the low solar wind ram pressure (Geotail is at more than 25 $R_E$).

[37] When the solar wind Alfvén Mach number is less than one, a spacecraft could be located in the inner far field region of the Alfvén wing. This spacecraft would then observe plasma speeds lower than in the solar wind, a magnetic field that points in a different direction (more aligned with the wing axis: $B_x$ and $B_y$ should be smaller), but the same field magnitude as in the solar wind. This ideal picture of an Alfvén wing only occurs sufficiently far from the magnetopause. Geotail however was always close to the magnetopause where slow mode waves and fast mode waves perturb the Alfvén wing: this region is called the foot of the Alfvén wing. In this region, the magnetic field magnitude, for instance, does not have to be the same as in the solar wind. In Figure 6, the inner foot region of the Alfvén wing is abbreviated IAW. Since the magnetic field data for these periods are not clearly visible in Figure 6 (due to the scale), a zoom is provided in Figure 7. In these regions, the observed decreasing trend in magnetic field magnitude indicates that Geotail was located in the foot of the inner part of the Alfvén wing. A decrease would not happen in the far field, where the field magnitude is expected to be essentially constant.

[38] For a solar wind Alfvén Mach number just slightly above one (implying $M_f$ just above one, see Appendix), the bow-shock is weak and located far away from the magnetopause. Consequently, the Alfvén waves generated at the Earth and propagating in the direction of the Alfvén characteristics are only partially affected by the fast mode waves generated far away by the shock. For these conditions, slightly modified Alfvén wings may be present inside of the magnetosheath. This means that a shock is present and that behind the bow-shock, the shocked magnetosheath interacts with the magnetopause to form a slightly modified Alfvén wing. If the Alfvén Mach number is sufficiently close to one, the slightly modified Alfvén wing is almost identical to a pure Alfvén wing. In Figure 6, the time periods where Geotail was in the inner foot region of the slightly modified Alfvén wing are striped in two colors abbreviated IAW/MSH.

[39] According to theoretical expectations [*Neubauer*, 1980] there should be no discontinuity between the inner Alfvén wing and the region of the outer Alfvén wing located upstream and downstream of the inner wings (as can be seen in Figure 1, bottom). However, there is a discontinuity everywhere toward the flanks (away from the plane of the drawing, not shown here). Therefore, we cannot exclude the possibility that during time intervals identified as periods when Geotail is located in the inner Alfvén wing, the spacecraft is actually located just upstream or just downstream of this inner Alfvén wing (but it cannot be situated on the flanks where the plasma speed, for instance, would be higher).

[40] The regions of Figure 6 abbreviated OAW correspond to peculiar time periods: while the velocity is higher at Geotail than at ACE, the magnetic field is weaker. In addition, $B_x$ is even sporadically positive during these periods. Although we do not know with certainty what happens during these intervals, we suggest as one possibility that Geotail may be located in the outer foot region of the Alfvén wing (OAW), on the flank, close to the inner foot region of the wing. During the third interval (around 12:30 UTC) it might be in the outer foot region of the slightly modified Alfvén wing (since $M_A$ is larger than one in the solar wind). The inner part of the Alfvén wing is an obstacle for the solar wind, when the plasma is partially deflected around the wing, it is accelerated on the flanks. This might explain why

**Figure 6.** Comparison between ACE and Geotail in situ data (first 10 panels); geomagnetic indices (3 bottom panels). Shown are the magnetic field and the plasma velocity in the GSE coordinate system, the position of Geotail (also in GSE: $X$ in red, $Y$ in green, $Z$ in blue and $r$ in black), the plasma density at ACE and the Alfvén Mach number at ACE, the AU and AL indices, the SYM-H index and the Kp index. The ACE data are shifted in time to account for the travel time between L1 and the Earth. The background colors indicate the regions where Geotail is located according to the legend situated above the first panel: solar wind (SW), magnetosheath (MSH), magnetosphere (MSP), the inner Alfvén wing (IAW) and the outer Alfvén wing (OAW).

**Table 1.** Minimum Variance Analysis for Alfvén Wing Boundary Crossings

| Date | Trans. Type | $\lambda_{int}/\lambda_{min}$ | **n** | Angle With AW |
|---|---|---|---|---|
| 25 May 2:38 UTC | IAW → OAW | 17.5 | (−0.14, −0.75, 0.65) | 85° |
| 25 May 7:01 UTC | IAW → OAW | 120.2 | (−0.37, −0.2, 0.91) | 59° |
| 25 May 8:12 UTC | IAW → OAW | 9.0 | (−0.16, 0.91, −0.38) | 69° |
| 25 May 12:28 UTC | IAW → OAW | 60.1 | (−0.38, −0.9, 0.23) | 83° |
| 25 May 12:38 UTC | OAW → IAW | 9.8 | (−0.27, −0.9, −0.33) | 90° |
| 25 May 12:42 UTC | OAW → IAW | 10.2 | (0.04, −0.89, 0.46) | 77° |
| 25 May 13:12 UTC | OAW → IAW | 15.4 | (0.42, 0.44, 0.8) | 81° |
| 25 May 16:03 UTC | IAW → OAW | 67.7 | (−0.08, −0.99, 0.07) | 76° |
| 25 May 16:04 UTC | OAW → IAW | 120.2 | (0.14, 0.94, −0.3) | 80° |

the plasma speed is higher at Geotail than at ACE. Moreover, outside the inner Alfvén wing the magnetic field is also perturbed, with the perturbation magnitude tapering off as described in section 2. As a result, on the outer Alfvén wing, in the region close to the inner Alfvén wing (where the magnetic field perturbation is the strongest), the magnetic field can be very different from the background magnetic field. This could explain the X-component of the magnetic field measured by Geotail. Another possibility would be that Geotail is situated close to the magnetopause, on the flank, where, due to the magnetic Lorentz force, strong flow accelerations occur when the solar wind Alfvén Mach number is low but not necessarily below one [see *Chen et al.*, 1993; *Lavraud et al.*, 2007].

[41] Figure 7 shows that during the period of very low density solar wind, the magnetic field magnitude at Geotail is lower than in the solar wind. This would be very unlikely if a strong bow-shock were present between ACE and Geotail. The details of the magnetic field configuration close to the magnetopause are complex and we do not know exactly how the Alfvén wings connect to the Earth's magnetic field and how the reconnection looks like in this case. It strongly depends, for instance, on the geometry and rate of intermittent reconnection at the magnetopause, similar to its occurrence at Ganymede [*Jia et al.*, 2010]. This could also contribute to the flow perturbations observed like the strong negative $v_z$ components.

[42] We have used the minimum variance analysis (MVA) [see *Sonnerup and Cahill*, 1967] to determine the normals to the discontinuities during Alfvén wing crossings. We then compare the direction of the normals with the direction of the wings given by $\mathbf{C}_{\mathbf{A}}^{\pm}$. While in the far field this normal should be perpendicular to the direction of the wing, this does not have to be exactly the case in the foot region. On 25 May 2002, we found 36 Alfvén wing crossings between 2:38 UTC and 16:04 UTC. For most of these crossings, the spacecraft is entering or leaving the Alfvén wing for only a very short amount of time. These events are therefore not always visible in Figures 6 and 7. For instance, Geotail left the IAW on 25 May 2002 at 16:02:55 UTC and came back inside the IAW at 16:03:47 UTC. The MVA gives satisfactory results with a well-defined normal only if the ratio of the intermediate to the minimum eigenvalue is large enough. In the present study, we only consider discontinuities where the ratio is larger than nine. This is the case for 9 of the 36 discontinuities. The results are summarized in Table 1, where we also indicate the type of discontinuity: IAW → OAW when the spacecraft is leaving the wing and OAW → IAW when the spacecraft is entering the wing. The last two columns of the table display the direction of the normal (**n**) and the angle between this normal and the direction of the wing, which should ideally be 90°. The ratio of the eigenvalues ($\lambda_{int}/\lambda_{min}$) are also given to indicate the quality of the results for each crossing. The angle between the normal and the direction of the wing is mostly close to 90° (more than 75° in 78% of the cases). This is in very good agreement with ideal Alfvén wing crossings, in particular if one considers the numerous uncertainties due to: the fact that Geotail is not in the far field region but rather in the foot of the Alfvén wing, that the MVA only gives an estimate for the direction of the normal (even though the ratios of the eigenvalues considered here are very high), and that values propagated from ACE are used to determine the orientation of the wing. It may also suggest that the establishment of the ideal, far field Alfvén wings occurs closer to magnetopause than expected.

[43] In a similar way, we also used the MVA to study the discontinuities when Geotail enters or leaves the closed magnetic field line region. We found 15 events and the ratios of the eigenvalues were large enough for 6 of them. The normals determined with this method are in good agreement with the magnetopause model of *Shue et al.* [1998].

## 5. Geomagnetic Activity

[44] The bottom panel of Figure 6 shows the geomagnetic activity indices Kp, AU, AL, and SYM-H (extracted from NASA/GSFC's OMNI data set through OMNIWeb). The Kp index measures geomagnetic activity on a global scale [*Bartels and Veldkamp*, 1949]. During 23 May 2002, before the Alfvén wing events, Kp values exceed 6, indicating a geomagnetic storm. The SYM-H index is similar to the Dst index but differs from it in the way the baseline is computed. In addition, the time resolution is different, while the Dst index is a 1h index, SYM-H is computed every minute. Like the Dst index, the SYM-H index essentially measures the energy content of the ring current [*Dessler and Parker*, 1959; *Sckopke*, 1966]. However, there are also contributions from other magnetospheric current systems, in particular from the Chapman-Ferraro currents in the magnetopause. On 23 May 2002, SYM-H shows a storm sudden commencement (SSC) starting at 10:50 UTC, followed by the main phase of a small storm beginning at 12:10 UTC, and intensifying to a moderate storm at 15:50 UTC with a minimum SYM-H of −115 nT. The storm begins to enter the recovery phase at ∼22:00 UTC on 23 May 2002. It is accompanied by strong substorm activities as can be seen in the AL and AU indices. However, by 00:00 UTC on 24 May 2002 all substorm activity ceases and there in no new substorm activity until late in 25 May

2002, well after the events of interest here. By contrast, the timescale of recovery of the storm is much less, and it does not conclude until after 25 May 2002. Thus, the events of interest here occur during the recovery phase of a small to moderate geomagnetic storm. Normally, the recovery phase of a storm still shows enhanced auroral activity. We have inspected IMAGE WIC images of auroral activity and found essentially none. We also inspected DMSP F13 passes over the polar caps and found much lower than normal electron and proton precipitation fluxes. Thus, during this low Alfvén Mach number event, the magnetosphere is geomagnetically extremely quiet, except for the enhanced ring current. The extreme quiescence of the polar ionosphere is not expected in view of the prevailing interplanetary magnetic field (IMF) conditions. Thus, the coupling mode between the magnetosphere and the ionosphere seems to be different from those during average times with higher Alfvén Mach number solar wind. This is probably related to the way IMF field lines connect to the polar ionosphere. Very little is known about this process, and Figure 4 only sketches this in the most general terms. A more elaborate discussion of the magnetosphere-ionosphere coupling (MI-coupling) process and of the variation of the ring current during sub-Alfvénic solar wind is beyond the scope of this observationally oriented paper; it would require, for instance, global simulations.

## 6. Discussions and Conclusions

[45] In this article, we presented several long time periods of up to four hours in May 2002 where the solar wind close to the Earth was sub-Alfvénic and sub-fast. During this interval of very low Alfvén Mach number, the magnetosphere was geomagnetically very quiet, except for the enhanced ring current and there was almost no auroral activity. Independent observations from multiple spacecraft show that the solar wind density was unexpectedly low for about 40 h. This low density led to a high Alfvén speed and sub-Alfvénic intervals. Theory predicts that, as a result, the bow-shock and the magnetosheath of the Earth disappeared and two Alfvén wings formed. In these wings, the plasma is decelerated and **B** and **v** experience a rotation. We estimated that the resulting structures were up to 600 $R_E$ long.

[46] In addition, we used in situ measurements from Geotail to search for Alfvén wing crossings. We found several time periods that are consistent with Geotail being located in the foot region of the wing. The evidence being: magnetic field displays a similar strength as in the solar wind but a different direction, the plasma velocity is lower than in the solar wind but higher than in the closed magnetic field line region, and the velocity direction is different from the solar wind velocity. Furthermore, using the MVA we determined the normals during nine Alfvén wing crossings. The direction of these normals were mostly perpendicular to the direction of the Alfvén wing, and therefore consistent with Alfvén wing crossings.

[47] Unfortunately, no spacecraft were located in the far field region of the Alfvén wing where purely Alfvénic perturbations are expected to occur. It can be seen, for instance, in the Geotail's measurements of the magnetic field magnitude, which jumps during Alfvén wing crossings: this would not likely be the case if Geotail were in the far field region.

[48] We found several time intervals where the plasma speed was higher at Geotail than at ACE and the magnetic field weaker. We do not know for certain which process may have generated such high plasma speeds. We suggest that Geotail was possibly located in the outer Alfvén wing, on the flank, where high velocities may occur, or close to the magnetopause, on the flank, where high velocity streams have already been observed during periods of low Alfvén Mach number incoming flow. It may also be due to the intermittent reconnection processes between the interplanetary magnetic field and the terrestrial magnetic field, analogous to the case of Ganymede albeit with a more complex geometry.

[49] How the reconnection between the solar wind and the magnetosphere was affected by these low density upstream conditions is not clear. The reconnection rate between two identical plasma displaying antiparallel magnetic fields is controlled by the Alfvén speed and the magnetic field magnitude [see *Parker*, 1973; *Birn et al.*, 2001]. When the magnetic fields are not parallel or when the two plasma are not identical (which is the case here on the day side magnetopause), the reconnection rate can be estimated, for instance, by equation (19) from *Cassak and Shay* [2007]. *Borovsky et al.* [2008] verified this equation by performing numerical simulations for a wide range of solar wind Alfvén Mach numbers ($1.9 < M_A < 16.3$). Since the plasma density for the event studied in the present paper is lower than usual, the reconnection rate should be higher than usual. Reconnection at the magnetopause of a body displaying Alfvén wings has already been studied for Ganymede by *Jia et al.* [2010]. This study demonstrates that at Ganymede's magnetopause, even though the background conditions are very steady, the reconnection is intermittent.

[50] Since the Earth's magnetosphere is completely different for sub-Alfvénic incoming flow, studying these rare events should help us to increase our understanding of the solar-terrestrial relationships.

[51] The very low density in the solar wind on 24 and 25 May 2002 may have its origin, for instance, in a long-lasting structure located on the Sun (low density events occurred almost periodically in 2002: 18 and 19 April, 20 March and 19 July) or may have been caused by a complex interaction of CMEs prior to the event (three halo CMEs reached the Earth on 23 May 2002). Further investigations are required to understand what generated this very low density solar wind.

[52] While sub-Alfvénic upstream conditions and Alfvén wings are very unusual for the planets of the solar system, they might be common for hot Jupiters, since these extrasolar planets are located very close to their stars. This was not the first time where the low solar wind density generated sub-Alfvénic conditions at the Earth: *Janardhan* [2006] studied the occurrence of solar wind disappearance events (density lower than 0.2 $cm^{-3}$) and found seven events between 1977 and 2002. Sub-Alfvénic solar wind conditions were measured, for instance, on 20 March 2002 ($M_A < 1$ for more than 2 h) or on 11 May 1999 ($M_A < 1$ for $\sim$1 h). These events will be inspected in details in a follow-up study. In addition, future solar wind conditions need to be monitored to find new occurrences of Alfvén wings at the Earth. If for one of these events, a spacecraft is located in the far field region, Alfvén wing crossings would be easier to identify than they are in the present study.

[53] The results obtained in the present paper encourage us to pursue this study with help of global numerical simulations. This will be the subject of future work and should improve our understanding of the dynamics of the system.

## Appendix A

[54] Using the definition of the fast mode wave velocity (see MHD textbooks [e.g., *Goedbloed and Poedts*, 2004]), taking the square of it and dividing it by the square of the plasma velocity, one can find the fast magnetosonic Mach number ($M_f$) at the apex of the bow-shock. It is given by:

$$M_f^{-2} = \frac{M_A^{-2}}{2}\left(1 + \frac{M_A^2}{M_{sd}^2} + \sqrt{\left(1 + \frac{M_A^2}{M_{sd}^2}\right)^2 - 4\frac{M_A^2}{M_{sd}^2}\cos^2\theta}\right), \quad \text{(A1)}$$

where $M_A$ and $M_{sd}$ are the Alfvén and sonic Mach number, respectively, and $\theta$ is the angle between the velocity and magnetic field vectors. For $\beta \ll 1$ (which implies $M_A^2 / M_{sd}^2 \ll 1$) we thus have $M_f \sim M_A$.

[55] **Acknowledgments.** The authors are grateful to Timo Grambusch, Sven Jacobsen, Olga Alexandrova and Alexandre Wennmacher for their assistance and Vytenis Vasyliūnas for helpful discussions. J.R. would like to thank Matthew Gilson for his assistance with the IMAGE data. These results were obtained within Schwerpunktprogramm "Planetary Magnetism" of die Deutsche Forschungsgemeinschaft under grant SA 1772/1-2 and within the framework of the following projects: GOA/2009-009 (K.U. Leuven), G.0729.11 (FWO-Vlaanderen) and C 90347 (ESA Prodex 9). The research leading to these results has also received funding from the European Commission's Seventh Framework Programme (FP7/2007-2013) under the grant agreements SOLSPANET (project 269299, www.solspanet.eu) and SPACECAST (project 262468, fp7-spacecast.eu). We thank the ACE, Genesis, Geotail, WIND and SOHO teams for making the data available.

[56] Robert Lysak thanks Jack Scudder and an anonymous reviewer for their assistance in evaluating this paper.

## References

Barraclough, B. L., et al. (2003), The Plasma Ion and Electron Instruments for the Genesis mission, *Space Sci. Rev.*, *105*, 627–660, doi:10.1023/A:1024426112422.

Bartels, J., and J. Veldkamp (1949), International data on magnetic disturbances, first quarter, 1949, *J. Geophys. Res.*, *54*, 295–299, doi:10.1029/JZ054i003p00295.

Bilitza, D. (2001), IRI 2000, *Radio Sci.*, *36*, 261–276, doi:10.1029/2000RS002432.

Bilitza, D., and B. W. Reinisch (2008), International Reference Ionosphere 2007: Improvements and new parameters, *Adv. Space Res.*, *42*, 599–609, doi:10.1016/j.asr.2007.07.048.

Birn, J., et al. (2001), Geospace Environmental Modeling (GEM) magnetic reconnection challenge, *J. Geophys. Res.*, *106*, 3715–3720, doi:10.1029/1999JA900449.

Borovsky, J. E., M. Hesse, J. Birn, and M. M. Kuznetsova (2008), What determines the reconnection rate at the dayside magnetosphere?, *J. Geophys. Res.*, *113*, A07210, doi:10.1029/2007JA012645.

Cassak, P. A., and M. A. Shay (2007), Scaling of asymmetric magnetic reconnection: General theory and collisional simulations, *Phys. Plasmas*, *14*(10), 102114, doi:10.1063/1.2795630.

Chao, J. K., D. J. Wu, C.-H. Lin, Y.-H. Yang, X. Y. Wang, M. Kessel, S. H. Chen, and R. P. Lepping (2002), Models for the size and shape of the Earth's magnetopause and bow shock, in *Space Weather Study Using Multipoint Techniques*, edited by L.-H. Lyu, pp. 127–135, Elsevier, New York.

Chen, S.-H., M. G. Kivelson, J. T. Gosling, R. J. Walker, and A. J. Lazarus (1993), Anomalous aspects of magnetosheath flow and of the shape and oscillations of the magnetopause during an interval of strongly northward interplanetary magnetic field, *J. Geophys. Res.*, *98*, 5727–5742, doi:10.1029/92JA02263.

Dessler, A. J., and E. N. Parker (1959), Hydromagnetic theory of geomagnetic storms, *J. Geophys. Res.*, *64*, 2239–2252, doi:10.1029/JZ064i012p02239.

Drell, S. D., H. M. Foley, and M. A. Ruderman (1965), Drag and propulsion of large satellites in the ionosphere: An Alfvén propulsion engine in space, *J. Geophys. Res.*, *70*, 3131–3145, doi:10.1029/JZ070i013p03131.

Fairfield, D. H. (1971), Average and unusual locations for the Earth's magnetopause and bow shock, *J. Geophys. Res.*, *76*, 6700–6716, doi:10.1029/JA076i028p06700.

Fairfield, D. H., I. H. Cairns, M. D. Desch, A. Szabo, A. J. Lazarus, and M. R. Aellig (2001), The location of low Mach number bow shocks at Earth, *J. Geophys. Res.*, *106*, 25,361–25,376, doi:10.1029/2000JA000252.

Farrugia, C. J., H. J. Singer, D. Evans, D. Berdichevsky, J. D. Scudder, K. W. Ogilvie, R. J. Fitzenreiter, and C. T. Russell (2000), Response of the equatorial and polar magnetosphere to the very tenuous solar wind on May 11, 1999, *Geophys. Res. Lett.*, *27*, 3773–3776, doi:10.1029/2000GL003800.

Frank, L. A., K. L. Ackerson, W. R. Paterson, J. A. Lee, M. R. English, and G. L. Pickett (1994), The Comprehensive Plasma Instrumentation (CPI) for the GEOTAIL spacecraft, *J. Geomagn. Geoelectr.*, *46*, 23–37.

Goedbloed, J. P. H., and S. Poedts (2004), *Principles of Magnetohydrodynamics*, Cambridge Univ. Press, Cambridge, U. K.

Hovestadt, D., et al. (1995), CELIAS - Charge, Element and Isotope Analysis System for SOHO, *Sol. Phys.*, *162*, 441–481, doi:10.1007/BF00733436.

Jacobsen, S., F. M. Neubauer, J. Saur, and N. Schilling (2007), Io's nonlinear MHD-wave field in the heterogeneous Jovian magnetosphere, *Geophys. Res. Lett.*, *341*, L10202, doi:10.1029/2006GL029187.

Janardhan, P. (2006), Enigmatic solar wind disappearance events - Do we understand them?, *J. Astrophys. Astron.*, *27*, 201–207.

Jia, X., R. J. Walker, M. G. Kivelson, K. K. Khurana, and J. A. Linker (2008), Three-dimensional MHD simulations of Ganymede's magnetosphere, *J. Geophys. Res.*, *113*, A06212, doi:10.1029/2007JA012748.

Jia, X., R. J. Walker, M. G. Kivelson, K. K. Khurana, and J. A. Linker (2010), Dynamics of Ganymede's magnetopause: Intermittent reconnection under steady external conditions, *J. Geophys. Res.*, *115*, A12202, doi:10.1029/2010JA015771.

Khurana, K. K., M. G. Kivelson, D. J. Stevenson, G. Schubert, C. T. Russell, R. J. Walker, and C. Polanskey (1998), Induced magnetic fields as evidence for subsurface oceans in Europa and Callisto, *Nature*, *395*, 777–780, doi:10.1038/27394.

Khurana, K. K., M. K. Dougherty, C. T. Russell, and J. S. Leisner (2007), Mass loading of Saturn's magnetosphere near Enceladus, *J. Geophys. Res.*, *112*, A08203, doi:10.1029/2006JA012110.

Kivelson, M. G., K. K. Khurana, C. T. Russell, R. J. Walker, J. Warnecke, F. V. Coroniti, C. Polanskey, D. J. Southwood, and G. Schubert (1996), Discovery of Ganymede's magnetic field by the Galileo spacecraft, *Nature*, *384*, 537–541, doi:10.1038/384537a0.

Kivelson, M. G., F. Bagenal, W. S. Kurth, F. M. Neubauer, C. Paranicas, and J. Saur (2004), Magnetospheric interactions with satellites, in *Jupiter: The Planet, Satellites and Magnetosphere*, edited by F. Bagenal, T. E. Dowling, and W. B. McKinnon, pp. 513–536, Cambridge Univ. Press, Cambridge, U. K.

Kokubun, S., T. Yamamoto, M. H. Acuña, K. Hayashi, K. Shiokawa, and H. Kawano (1994), The GEOTAIL magnetic field experiment, *J. Geomagn. Geoelectr.*, *46*, 7–21.

Lavraud, B., J. E. Borovsky, A. J. Ridley, E. W. Pogue, M. F. Thomsen, H. Rème, A. N. Fazakerley, and E. A. Lucek (2007), Strong bulk plasma acceleration in Earth's magnetosheath: A magnetic slingshot effect?, *Geophys. Res. Lett.*, *34*, L14102, doi:10.1029/2007GL030024.

Le, G., C. T. Russell, and S. M. Petrinec (2000), The magnetosphere on May 11, 1999, the day the solar wind almost disappeared: I. Current systems, *Geophys. Res. Lett.*, *27*, 1827–1830, doi:10.1029/1999GL010774.

Lepping, R. P., et al. (1995), The Wind Magnetic Field Investigation, *Space Sci. Rev.*, *71*, 207–229, doi:10.1007/BF00751330.

Lin, R. P., et al. (1995), A three-dimensional plasma and energetic particle investigation for the Wind spacecraft, *Space Sci. Rev.*, *71*, 125–153, doi:10.1007/BF00751328.

Linker, J. A., M. G. Kivelson, and R. J. Walker (1991), A three-dimensional MHD simulation of plasma flow past Io, *J. Geophys. Res.*, *962*, 21,037–21,053, doi:10.1029/91JA02132.

McComas, D. J., S. J. Bame, P. Barker, W. C. Feldman, J. L. Phillips, P. Riley, and J. W. Griffee (1998), Solar Wind Electron Proton Alpha Monitor (SWEPAM) for the Advanced Composition Explorer, *Space Sci. Rev.*, *86*, 563–612, doi:10.1023/A:1005040232597.

Mukai, T., S. Machida, Y. Saito, M. Hirahara, T. terasawa, N. Kaya, and T. Obara (1994), The Low Energy Particle (LEP) Experiment onboard the GEOTAIL satellite, *J. Geomagn. Geoelectr.*, *46*, 669–692.

Neubauer, F. M. (1980), Nonlinear standing Alfven wave current system at Io: Theory, *J. Geophys. Res.*, *85*, 1171–1178, doi:10.1029/JA085iA03p01171.

Neubauer, F. M. (1998), The sub-Alfvénic interaction of the Galilean satellites with the Jovian magnetosphere, *J. Geophys. Res.*, *103*, 19,843–19,866, doi:10.1029/97JE03370.

Parker, E. N. (1973), The reconnection rate of magnetic fields, *Astrophys. J.*, *180*, 247–252, doi:10.1086/151959.

Ridley, A. J. (2007), Alfvén wings at Earth's magnetosphere under strong interplanetary magnetic fields, *Ann. Geophys.*, *25*, 533–542, doi:10.5194/angeo-25-533-2007.

Russell, C. T., G. Le, P. Chi, X.-W. Zhou, J.-H. Shue, S. M. Petrinec, P. Song, F. R. Fenrich, and J. G. Luhmann (2000), The extreme compression of the magnetosphere on May 4, 1998, as observed by the Polar spacecraft, *Adv. Space Res.*, *25*, 1369–1375, doi:10.1016/S0273-1177(99)00646-8.

Saur, J., F. M. Neubauer, D. F. Strobel, and M. E. Summers (1999), Three-dimensional plasma simulation of Io's interaction with the Io plasma torus: Asymmetric plasma flow, *J. Geophys. Res.*, *1042*, 25,105–25,126, doi:10.1029/1999JA900304.

Schilling, N., F. M. Neubauer, and J. Saur (2007), Time-varying interaction of Europa with the jovian magnetosphere: Constraints on the conductivity of Europa's subsurface ocean, *Icarus*, *192*, 41–55, doi:10.1016/j.icarus.2007.06.02.

Schunk, R. W., and A. F. Nagy (2000), Ionospheres: Physics, Plasma Physics, and Chemistry, Cambridge Univ. Press, Cambridge, U. K.

Sckopke, N. (1966), A general relation between the energy of trapped particles and the disturbance field near the Earth, *J. Geophys. Res.*, *71*, 3125–3130.

Shkolnik, E., G. A. H. Walker, and D. A. Bohlender (2003), Evidence for Planet-induced Chromospheric Activity on HD 179949, *Astrophys. J.*, *597*, 1092–1096, doi:10.1086/378583.

Shue, J.-H., et al. (1998), Magnetopause location under extreme solar wind conditions, *J. Geophys. Res.*, *1031*, 17,691–17,700, doi:10.1029/98JA01103.

Smith, C. W., J. L'Heureux, N. F. Ness, M. H. Acuña, L. F. Burlaga, and J. Scheifele (1998), The ACE Magnetic Fields Experiment, *Space Sci. Rev.*, *86*, 613–632, doi:10.1023/A:1005092216668.

Sonnerup, B. U. O., and L. J. Cahill, Jr. (1967), Magnetopause structure and attitude from Explorer 12 observations, *J. Geophys. Res.*, *72*, 171–183, doi:10.1029/JZ072i001p00171.

Terasawa, T., et al. (2000), GEOTAIL observations of anomalously low density plasma in the magnetosheath, *Geophys. Res. Lett.*, *27*, 3781–3784, doi:10.1029/2000GL000087.

Wolf-Gladrow, D. A., F. M. Neubauer, and M. Lussem (1987), Io's interaction with the plasma torus: A self-consistent model, *J. Geophys. Res.*, *92*, 9949–9961, doi:10.1029/JA092iA09p09949.